Davenport, J. B., & Fisher, L. R. (1975) *Chem. Phys. Lipids 14*, 275–290.
DeBose, C. D., & Roberts, M. F. (1983) *J. Biol. Chem. 258*, 6327–6334.
Dluhy, R. A., Cameron, D. G., Mantsch, H. H., & Mendelsohn, R. A. (1983) *Biochemistry 22*, 6318–6325.
Eaton, B. R., & Dennis, E. A. (1976) *Arch. Biochem. Biophys. 176*, 604–609.
Eliasz, A. W., Chapman, D., & Ewing, D. F. (1976) *Biochim. Biophys. Acta 448*, 220–230.
Fringel, U. P., & Gunthard, H. (1976) *Biochim. Biophys. Acta 450*, 101–106.
Gabriel, N. E., & Roberts, M. F. (1984) *Biochemistry 23*, 4011–4015.
Gregoriadis, G., Ed. (1984) *Liposome Technology*, Vol. 1, CRC Press, Boca Raton, FL.
Hamilton, R., Jr., Goerke, L., Guo, L., Williams, M., & Havel, R. (1980) *J. Lipid Res. 21*, 981–992.
Hauser, H., Gains, N., & Mueller, M. (1983) *Biochemistry 22*, 4775–4781.
Kensil, C. A., & Dennis, E. A. (1979) *J. Biol. Chem. 254*, 5843–5848.
Kitagawa, T., Tanaka, K. I., & Nojima, S. (1977) *Biochim. Biophys. Acta 467*, 137–145.
Mabrey, S., & Sturtevant, J. M. (1978) *Methods Membr. Biol. 9*, 237–274.
Mantsch, H. H. (1984) *J. Mol. Struct. 113*, 201–212.
Papahadjopoulos, D., & Watkins, J. C. (1967) *Biochim. Biophys. Acta 135*, 639–650.
Papahadjopoulos, D., & Kimelberg, H. K. (1973) *Prog. Surf. Sci. 4*, 139–221.
Racker, E., & Stoeckenius, W. (1974) *J. Biol. Chem. 249*, 660–663.
Reman, F. C., Demel, R. A., de Gier, J., van Deenen, L. L. M., Eibl, H., & Westphal, O. (1969) *Chem. Phys. Lipids 3*, 221–233.
Ruocco, M. J., Siminovitch, D. J., & Griffin, R. G. (1985) *Biochemistry 24*, 2406–2411.
Ryman, B. E., & Tyrrell, D. A. (1980) in *Essays in Biochemistry* (Campbell, P. N., & Marshall, R. D., Eds.) pp 49–98, Academic Press, London.
Seelig, J. (1978) *Biochim. Biophys. Acta 515*, 105–140.
Shinitzky, M., & Barenholz, Y. (1974) *J. Biol. Chem. 249*, 2652–2657.
Snyder, R. G., Hsu, S. L., & Krimm, S. (1978) *Spectrochim. Acta, Part A 34A*, 395–406.
Stockton, G. W., Polnaszek, C. F., Tulloch, A. D., Hasan, F., & Smith, I. C. P. (1976) *Biochemistry 15*, 954–966.
Tausk, R. J. M., Oudshoorn, C., & Overbeek, J. Th. G. (1974) *Biophys. Chem. 2*, 53–63.
Urbaneja, M., Arrondo, J. R., Alonso, A., & Goni, F. M. (1985) in *Surfactants in Solution* (Mittal, K. L., Ed.) Vol. 5, Plenum Press, New York.

Conformation and Stability of the Constant Fragment of the Immunoglobulin Light Chain Containing an Intramolecular Mercury Bridge

Yuji Goto and Kozo Hamaguchi*
Department of Biology, Faculty of Science, Osaka University, Toyonaka, Osaka 560, Japan
Received June 18, 1985; Revised Manuscript Received November 5, 1985

ABSTRACT: The constant fragment of the immunoglobulin light chain in which the intramolecular disulfide bond is reduced (reduced C_L fragment) assumes a conformation very similar to that of the intact C_L fragment and contains two sulfhydryl groups buried in the interior of the molecule [Goto, Y., & Hamaguchi, K. (1979) *J. Biochem. (Tokyo) 86*, 1433–1441]. In order to understand the role of the disulfide bond, a derivative in which the disulfide bond is replaced by an S–Hg–S bond was prepared and its conformation and stability were studied. The derivative was prepared by reacting the reduced C_L fragment with mercuric chloride. Kinetic studies showed that the reaction is rate-limited by the unfolding process of the reduced C_L fragment. The mercury derivative was as compact as the intact C_L or reduced C_L fragment, and a tryptophyl residue was found to be buried near the S–Hg–S bond in the interior of the protein molecule. Judging from the circular dichroic spectrum, however, the β-structure characteristic of the immunoglobulin fold was disturbed. The stability of the derivative to guanidine hydrochloride was lower than that of the intact C_L fragment, but the unfolding transition was reversible and cooperative. Decreased stability of the mercury derivative is due to its folded conformation being distorted by introduction of the S–Hg–S bond.

The protein molecule forms a unique three-dimensional structure determined by its primary structure. Elucidation of the pathway by which the three-dimensional structure of a protein molecule is built up is essential for understanding the structure and function of the protein. We have studied the pathway of protein folding experimentally using the isolated domains of immunoglobulin (Goto et al., 1979; Goto & Hamaguchi, 1979, 1981, 1982a,b; Sumi & Hamaguchi, 1982; Ashikari et al., 1985). Each domain of the immunoglobulin molecule consists of about 110 amino acid residues and has only one intrachain disulfide bond buried in the interior hydrophobic region between two β-sheets (Davies et al., 1975; Amzel & Poljak, 1979). The loop formed by the disulfide bond consists of 60 amino acid residues. The conformations of the domains are retained intact even when they are isolated as fragments. Intrachain disulfide bonds play a decisive role in determining the three-dimensional structures of many proteins. Therefore, the immunoglobulin domain may be

0006-2960/86/0425-2821$01.50/0

regarded as a suitable protein for studying the pathway of protein folding in relation to the role of the intrachain disulfide bond.

We first compared the conformation and stability of the reduced C_L fragment with those of the intact C_L fragment and found that the former assumes a conformation very similar to but with a lower stability than that of the latter (Goto & Hamaguchi, 1979). We compared kinetics of unfolding and refolding of the intact C_L and reduced C_L fragments in Gdn-HCl and showed that the disulfide bond increases the folding rate but changes the unfolding rate only a little (Goto & Hamaguchi, 1982a,b). We also studied formation of the intrachain disulfide bond in the reduced C_L fragment in the presence of glutathione (Goto & Hamaguchi, 1981) and showed that exposure of the two SH groups by unfolding of the reduced C_L fragment is necessary for the formation of the disulfide bond. We pointed out the possibility that the formation of disulfide bonds of other reduced proteins is determined not only by the proximity of each pair of cysteinyl residues by conformational transitions but also by the unreactivities of cysteinyl residues owing to burial in the molecular interior of intermediates formed during the refolding process. Recently Ashikari et al. (1985) studied alkaline denaturation of the C_L fragment and clarified the effect of ionization of SH groups on stability of the reduced C_L fragment.

To understand further the role of disulfide bonds, we prepared a derivative of the C_L fragment in which the disulfide bond is replaced by an S–Hg–S bond. Insertion of mercury increases the length of the disulfide bond by 3 Å (Bradley & Kunchur, 1965). In this paper, we describe the conformation and stability of the derivative. It was found that the β-sheet structure of the C_L fragment is disturbed by the introduction of the S–Hg–S bond but that the conformation of the derivative is as compact as that of the intact C_L fragment. Stability of the derivative to Gdn-HCl and heat is lower than that of the intact C_L fragment.

Materials and Methods

Materials. Bence-Jones protein (Nag, type λ) dimer was prepared as previously described (Goto et al., 1979), and the C_L fragment of the protein was obtained by digestion with papain (Goto & Hamaguchi, 1979). The reduced C_L fragment was prepared by reduction of the intrachain disulfide bond of the C_L fragment with 20 mM dithiothreitol in the presence of 4 M Gdn-HCl and then separated from the residual reagents on a column of Sephadex G-25 equilibrated with an acetate buffer at pH 5 (Goto & Hamaguchi, 1979). Bovine serum albumin, ovalbumin, bovine erythrocyte carbonic anhydrase, bovine pancreatic α-chymotrypsinogen A (type II), equine skeletal muscle myoglobin (type I), bovine pancreatic ribonuclease A (type I-A), and horse heart cytochrome *c* (type III) were obtained from Sigma Chemical Co. Bovine pancreatic trypsin inhibitor was kindly provided by Prof. T. Ikenaka of Osaka University. Gdn-HCl (specifically purified grade), mercuric chloride, DTNB, DTT, and other reagents were obtained from Nakarai Pure Chemicals Co. and were used without further purification.

CD Measurement. All measurements in this study were carried out at pH 7.5. For measurements at 25 °C, 50 mM Tris-HCl buffer containing 0.15 M NaCl or 10 mM sodium phosphate buffer containing 0.15 M NaCl was used. There was no difference between the results obtained with the two buffer systems. For measurements of thermal unfolding, 10 mM sodium phosphate buffer containing 0.15 M NaCl was used. All the buffer solutions were degassed before use.

CD measurements were carried out with a Jasco spectropolarimeter, Model J-500A, equipped with a DP-501 data processor. The CD instrument was calibrated with *d*-10-camphorsulfonic acid. The results are expressed as mean residue ellipticity, $[\theta]$, which is defined as $[\theta] = 100\,\theta_{obsd}/(lc)$, where θ_{obsd} is the observed ellipticity in degrees, c is the concentration in residue moles per liter, and l is the length of the light path in centimeters. For calculation of c, a value of 108 was used as the mean residue molecular weight. CD spectra were measured at a protein concentration of about 0.2 mg/mL with a 2.0-cm cell from 320 to 250 nm and with a 0.1-cm cell from 250 to 200 nm. The temperature was controlled at 25 °C with a thermostatically controlled cell holder. Thermal unfolding of the C_L-Hg fragment[1] was measured at 270 nm, because the change in the ellipticity in the far-ultraviolet region was small (see Figure 5). The protein concentration was 0.05 mg/mL, and a 2.0-cm cell was used. Thermal unfolding of the intact C_L and reduced C_L was measured at 218 nm. The protein concentrations were 0.05 mg/mL, and a 0.5-cm cell was used. The temperature was continuously increased at a rate of 0.5 °C/min and was measured with a calibrated copper–Constantan thermocouple.

Fluorescence Measurement. Fluorescence was measured with a Hitachi fluorescence spectrophotometer, Model MPF-4, equipped with a spectral corrector. Tryptophyl fluorescence was measured by using 280-nm light for excitation. The protein concentration was about 0.02 mg/mL. The temperature was kept at 25 °C with a thermostatically controlled cell holder.

Ultraviolet Absorption Measurement. The difference absorption spectrum of the C_L-Hg fragment vs. reduced C_L fragment was recorded with a Cary Model 118 spectrophotometer. Protein concentration was 0.25 mg/mL. The change in the molar extinction coefficient ($\Delta\epsilon$) was calculated assuming the molecular weight to be 11 500. The absorption spectrum of the S–Hg–S bond was determined by measuring the difference absorption for the reaction of the reduced glutathione with mercuric chloride. The concentrations of reduced glutathione and mercuric chloride were 2.0 and 0.5 mM, respectively. The temperature was kept at 25 °C with a thermostatically controlled cell holder.

Titration of SH Groups with DTNB. The SH content of the reduced C_L fragment in the absence of mercuric chloride was checked by titration with DTNB after each spectroscopic measurement as described previously (Goto & Hamaguchi, 1979). It was always between 1.9 and 2.1.

The SH contents of the reduced C_L fragment in the presence of mercuric ions at various concentrations were determined by titration with DTNB. The titration in the absence of denaturant was carried out as follows. A mixture of the reduced C_L fragment and mercuric chloride at a given concentration in Tris-HCl buffer at pH 7.5 was incubated overnight at 25 °C. To 2.5 mL of the solution was added 0.5 mL of freshly prepared DTNB solution (3 mM) in the same buffer. The solution was left for another hour at 25 °C to complete the titration because of the slow titration of the SH groups of the reduced C_L fragment in the absence of denaturant (Goto & Hamaguchi, 1979). Then the absorption at 412 nm was measured against a reagent blank by using a Hitachi Model

[1] Abbreviations: C_L-Hg fragment, the constant fragment of the immunoglobulin light chain (C_L) in which the intrachain disulfide bond is replaced by the bond S–Hg–S; reduced C_L fragment, C_L fragment in which the intrachain disulfide bond is reduced; CD, circular dichroism; DNP-alanine, 2,4-dinitrophenylalanine; DTNB, 5,5′-dithiobis(2-nitrobenzoic acid); DTT, dithiothreitol; Gdn-HCl, guanidine hydrochloride; Tris, tris(hydroxymethyl)aminomethane.

Table I: Spectroscopic Properties and Stokes Radii of the C_L Fragment and Its Modified Forms at pH 7.5 and 25 °C

protein	min in CD from 200 to 250 nm ([θ] at min)[a]	max in tryptophyl fluorescence (rel fluorescence at max)	difference absorption at ~293 nm (wavelength at min)[b]	Stokes radius (Å)
intact C_L	218 nm (−7300)	325 nm (35)		18
reduced C_L	216 nm (−7000)	330 nm (80)	−750 (295 nm)	18
C_L-Hg	220 nm (−4300)	335 nm (25)	−100 (292 nm)	19
reduced and alkylated C_L		350 nm (90)	−2500 (293 nm)	24
C_L in 4 M Gdn-HCl		350 nm (100)		30[c]

[a] In deg cm^2 dmol^{-1}. [b] Against the absorption of intact C_L fragment, in M^{-1} cm^{-1}. [c] The value calculated by using the equation $[\eta] = 0.716n^{0.66}$, where $[\eta]$ is the intrinsic viscosity and n is the number of residues (Tanford, 1970), and eq 1.

323 spectrophotometer. The titration in the presence of 3 M Gdn-HCl was carried out in a similar way. A mixture of the reduced C_L fragment and mercuric chloride in 3 M Gdn-HCl was left for 1 h, and the SH content was titrated immediately after the addition of DTNB because of the rapid reaction of the SH groups in the unfolded molecule. The molar extinction coefficient of the reduced DTNB was assumed to be 13 600 M^{-1} cm^{-1} at 412 nm (Ellman, 1958; Gething & Davidson, 1972).

Analytical Gel Filtration. Analytical gel filtration was carried out on a Sephadex G-75 column (1 × 110 cm). The column was calibrated with the following nine proteins with the Stokes radii shown in parentheses: cytochrome *c* (17 Å), ribonuclease A (17.5 Å), myoglobin (19 Å), α-chymotrypsinogen (22 Å), carbonic anhydrase (24 Å), ovalbumin (28 Å), bovine serum albumin (34 Å), Bence-Jones protein dimer (29 Å), and bovine pancreatic trypsin inhibitor (16.5 Å). The Stokes radii of cytochrome *c*, ribonuclease A, myoglobin, and ovalbumin are the values calculated by Le Maire et al. (1980) using sedimentation coefficients; the radius of pancreatic trypsin inhibitor was calculated by using the diffusion coefficient (Squire & Himmel, 1979); the radius of the Bence-Jones protein dimer was determined by gel chromatography (Karlsson et al., 1972); and the radii of α-chymotrypsinogen, carbonic anhydrase, and serum albumin were calculated by using the intrinsic viscosity $[\eta]$ given by Tanford (1968)

$$[\eta] = (2.5N/M_r)(4/3\pi R_S^3) \quad (1)$$

where R_S is the Stokes radius, N is Avogadro's number, and M_r is the molecular weight.

To the column equilibrated with sodium phosphate buffer at pH 7.5 was added 0.5 mL of the solution of each protein in the same buffer. Each applied solution contained 0.5 mg of protein, 0.3 mg of blue dextran, and 0.05 mg of DNP-alanine. The column was thermostatically controlled at 25 °C by circulating water. Fractions of 1 mL were collected at a flow rate of 4 mL/h, and the absorbance at 280 nm of the eluate was measured. The partition coefficient (K_d) of each protein was obtained by the relation $K_d = (V_e - V_0)/(V_t - V_0)$, where V_e, V_0, and V_t are the elution volume of the protein, void volume, and total volume of the column, respectively. For the values of V_0 and V_t, we used the elution volumes of blue dextran and DNP-alanine, respectively. Under these experimental conditions, DNP-alanine was found not to be adsorbed onto Sephadex G-75.

Protein Concentration. Protein concentration was determined spectrophotometrically. The absorption coefficients at 280 nm for a 1% (w/v) solution in a 1.0-cm cell ($A^{1\%}_{1\,cm}$) of the intact C_L and reduced C_L fragments were assumed to be 14.6 and 14.5, respectively (Goto & Hamaguchi, 1979). The value of the C_L-Hg fragment was assumed to be the same as that of the reduced C_L fragment.

pH Measurement. pH was measured with a Radiometer PHM26c at 25 °C.

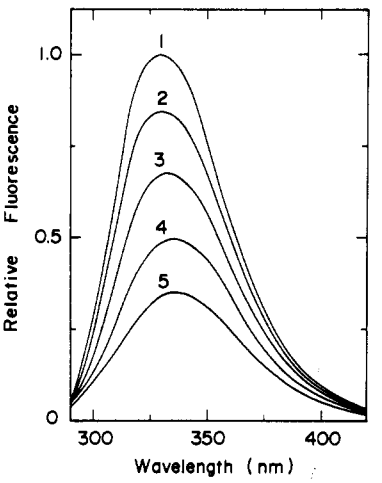

FIGURE 1: Fluorescence spectra of the reduced C_L fragment (1) and the reduced C_L fragment in the presence of 0.25 (2), 0.5 (3), 0.75 (4), and 1.0 mol (5) of mercuric ion per mole of the C_L fragment at pH 7.5 and 25 °C. The solutions were left overnight before measurements were taken. The protein concentration was 0.02 mg/mL. Excitation was at 280 nm.

RESULTS

Reaction of the Reduced C_L Fragment with Mercuric Ions. Figure 1 shows the fluorescence spectra of the reduced C_L fragment in the presence of mercuric chloride at various concentrations. An increase in the concentration of mercuric chloride decreased the fluorescence intensity of the reduced C_L fragment. A plot of the fluorescence intensity at 330 nm against the concentration of mercuric ions (Figure 2a) gave a curve with a sharp break at the molar ratio $[Hg^{2+}]/[C_L] = 1.0$. This indicates that 1 mol of mercuric ion interacts specifically with 1 mol of the reduced C_L fragment. The fluorescence intensity decreased by 70%, and the maximum wavelength shifted by 5 nm to a longer wavelength (335 nm) on interaction (Table I).

We also examined the change in the SH content accompanying the reaction. The SH contents of the reduced C_L fragment in the presence of mercuric ions at various concentrations are shown in Figure 2b. While 2 mol of SH group was titrated with DTNB in the absence of mercuric ions, the SH content decreased with increasing mercuric ion concentration, and no SH group was titrated when 1 mol or more of mercuric ions was added per mole of the reduced C_L fragment. The titration curve was the same as that determined by fluorescence quenching. This result shows that one mercuric ion reacts specifically with a pair of cysteinyl residues of the reduced C_L fragment.

Figure 3 shows the kinetics of the reaction of the reduced C_L fragment with mercuric ions at the molar ratio $[Hg^{2+}]/[C_L] = 1.5$ measured by the fluorescence change at 330 nm. The reaction was slow, and the whole process of quenching was observed. The reaction followed first-order kinetics with

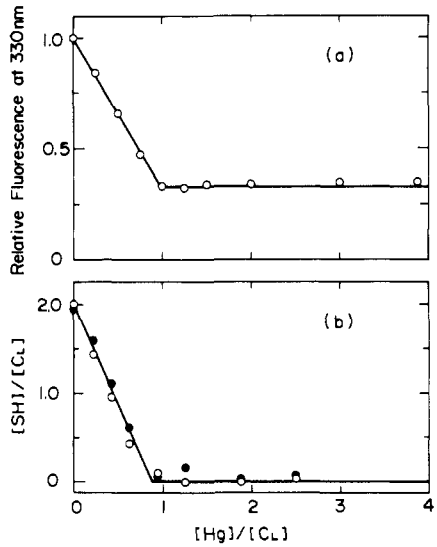

FIGURE 2: Titration with mercuric ions of the fluorescence at 330 nm (a) and of the SH content (b) of the reduced C_L fragment at pH 7.5 and 25 °C. (a) Excitation was at 280 nm, and the protein concentration was 0.02 mg/mL. (b) (○) In the absence of denaturant; (●) in the presence of 3 M Gdn-HCl. The protein concentration was 0.1 mg/mL.

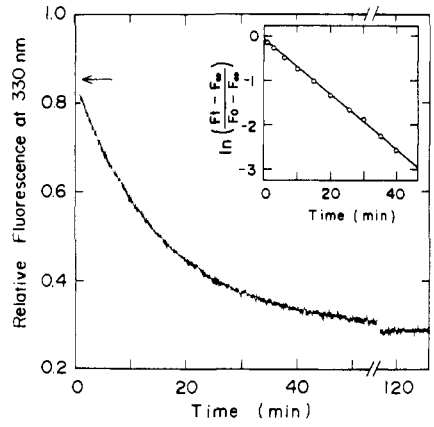

FIGURE 3: Kinetics of the reaction of the reduced C_L fragment with mercuric ions at pH 7.5 and 25 °C. To 2.5 mL of solution of the reduced C_L fragment was added 0.1 mL of solution of mercuric chloride, and the fluorescence change at 330 nm with time was measured. Excitation was at 280 nm. The arrow indicates the fluorescence intensity of the reduced C_L fragment in the absence of mercuric chloride. The final concentrations of the reduced C_L fragment and mercuric chloride were 1.8 and 2.7 μM, respectively. The inset shows the first-order plot of the kinetics.

an apparent rate constant of 1.1×10^{-3} s^{-1} (see inset of Figure 3). The kinetics were independent of the concentration of mercuric ions, and the same first-order rate constant was obtained in the range of 1–6 mol of mercuric ions/mol of the C_L fragment (not shown). The rate constant of the reaction of the reduced C_L fragment with mercuric ions was the same as the unfolding rate of the reduced C_L fragment determined previously under the same conditions (Goto & Hamaguchi, 1982b). These findings indicate that the SH groups buried in the interior of the reduced C_L fragment cannot react with mercuric ions and that the reaction is rate-limited by the exposure of the SH groups as a result of unfolding (see Discussion). This further suggests that the reaction of mercuric ions with the pair of SH groups to form the S–Hg–S bond occurs in the unfolded state of the reduced C_L fragment in water.

We next examined the reaction in the presence of 3 M Gdn-HCl, which has the effect of unfolding the reduced C_L fragment, so that the interaction between the unfolded C_L fragment and mercuric ions can be studied. We titrated the SH groups of the reduced C_L fragment with DTNB in the presence of mercuric ions at various concentrations in 3 M Gdn-HCl. As shown in Figure 2b, 1 mol of mercuric ion reacted with 2 mol of SH group. This shows that the intramolecular S–Hg–S bond is formed exclusively even in the unfolded state. As described below, the C_L-Hg fragment prepared in the presence of 3 M Gdn-HCl was indistinguishable from that prepared in water and then denatured by Gdn-HCl.

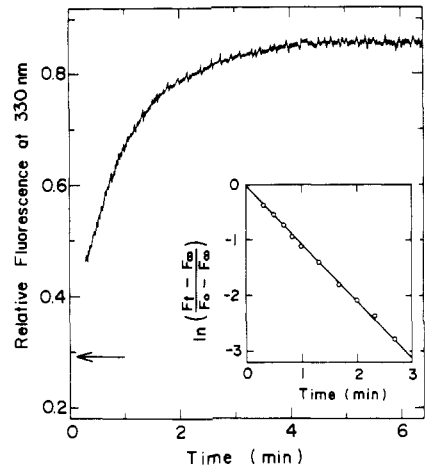

FIGURE 4: Kinetics for reaction of the C_L-Hg fragment with DTT measured by fluorescence at 330 nm at pH 7.5 and 25 °C. Concentrations of the C_L-Hg fragment and DTT were 2 μM and 3.5 mM, respectively. The arrow indicates the value for the C_L-Hg fragment. The inset shows the first-order plot of the kinetics.

Reaction of the C_L-Hg Fragment with DTT. In the following studies, we used the C_L-Hg fragment prepared in water in the presence of 1.2 mol of mercuric ion/mol of reduced C_L fragment.

We found that the S–Hg–S bond of the C_L-Hg fragment was reduced with DTT. Figure 4 shows the reaction of 2 μM C_L-Hg fragment with 3.5 mM DTT at pH 7.5 as measured by fluorescence at 330 nm. The fluorescence increased with time after the addition of DTT with an apparent first-order rate constant of 0.017 s^{-1}. The fluorescence spectrum after equilibration had a maximum at 330 nm and was identical with the spectrum of the reduced C_L fragment. This shows that the reduced C_L fragment was regenerated by the reaction of the C_L-Hg fragment with DTT. The mercury ion is removed from the C_L-Hg fragment and forms a circular complex with DTT. To understand the mechanism of the reaction, we examined the reactions at various concentrations of DTT. The kinetics were almost independent of the concentration of DTT in the concentration range of 1–20 mM. This shows that the S–Hg–S bond of the C_L-Hg fragment is buried in the interior of the molecule and that the reaction with DTT is rate-limited by the exposure of the S–Hg–S bond by the intramolecular fluctuation.

CD Spectra. Figure 5 shows the CD spectra of the C_L-Hg fragment in the absence and presence of 4 M Gdn-HCl, as well as the CD spectra of the intact C_L, reduced C_L, and reduced and alkylated C_L fragments. We showed previously (Goto & Hamaguchi, 1979) that the CD spectrum of the reduced C_L fragment is very similar in the far-ultraviolet region to that of the intact C_L fragment but that the spectrum of the reduced and alkylated C_L fragment differs greatly from that of the intact C_L fragment. The CD spectrum of the C_L-Hg fragment in this region in the absence of denaturant was

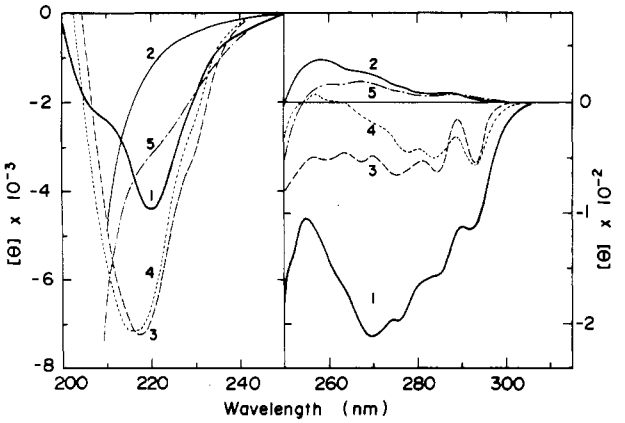

FIGURE 5: CD spectra of the C_L-Hg fragment in the absence (1) and presence (2) of 4 M Gdn-HCl at pH 7.5 and 25 °C. Protein concentration was 0.2 mg/mL. Curves 3, 4, and 5 show the CD spectra of the intact C_L, reduced C_L, and reduced and alkylated C_L fragments, respectively, cited from a previous paper (Goto & Hamaguchi, 1979).

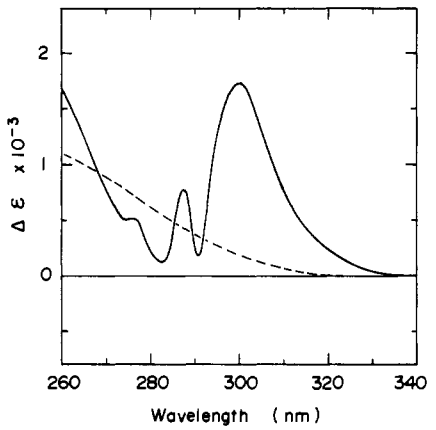

FIGURE 6: Difference absorption spectra of the C_L-Hg fragment vs. intact C_L fragment (solid line) and the complex of reduced glutathione with mercury vs. reduced glutathione (broken line) at pH 7.5 and 25 °C. Concentrations of the C_L fragment and glutathione were 0.3 and 0.2 mg/mL, respectively.

different from that of the intact C_L or reduced C_L fragment. It had a negative maximum at 220 nm and a shoulder at around 207 nm. The ellipticity at the minimum (−4300 deg cm^2 dmol^{-1}) was smaller than that of the intact C_L or reduced C_L fragment (about −7000 deg cm^2 dmol^{-1}) (Table I). This indicates that the β-sheet conformation of the C_L fragment is disturbed and that a different secondary structure is formed in the C_L-Hg fragment. In the region of 250–300 nm, the ellipticity of the C_L-Hg fragment in the absence of denaturant was more negative than those of the other forms of the C_L fragment. The ellipticity at 270 nm was −200 deg cm^2 dmol^{-1}, which is about 3 times larger than that of the intact C_L fragment. The negative CD bands at around 270 and 220 nm disappeared as a result of the unfolding of the C_L-Hg fragment by 4 M Gdn-HCl, and the spectrum was similar to those of the other C_L fragments in 4 M Gdn-HCl.

Difference Absorption Spectra. The state of the tryptophyl residues in the C_L-Hg fragment was studied by means of difference absorption spectroscopy. Figure 6 shows the difference spectrum of the C_L-Hg fragment vs. reduced C_L fragment. Also shown in this figure is the absorption spectrum of the S–Hg–S bond obtained by measuring the difference absorption for the reaction of reduced glutathione with mercuric ions. The difference spectrum of the C_L-Hg fragment vs. reduced C_L fragment had a large positive peak at 300 nm with a $\Delta\epsilon$ value of +1700 cm^{-1} M^{-1}. The absorption of the

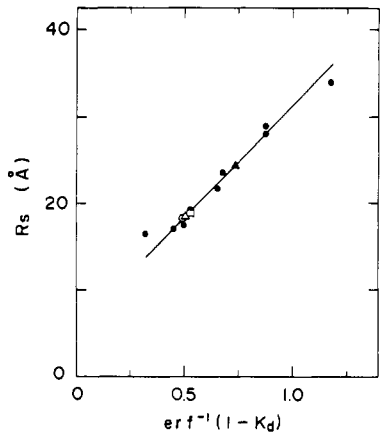

FIGURE 7: Analytical gel filtration of the intact C_L (○), reduced C_L (△), C_L-Hg (□), and reduced and alkylated C_L (▲) fragments on a Sephadex G-75 column (1 × 110 cm) at pH 7.5 and 25 °C. The ordinate represents the Stokes radius and the abscissa the inverse error function of $(1 - K_d)$. The column was calibrated with nine standard proteins (●) according to the smallest to the largest Stokes radius; these were pancreatic trypsin inhibitor, cytochrome *c*, ribonuclease A, myoglobin, α-chymotrypsinogen, carbonic anhydrase, Bence-Jones protein dimer, ovalbumin, and serum albumin. See text for details.

S–Hg–S bond was small, and no peak was observed at 300 nm. Thus the positive peak at 300 nm observed for the C_L-Hg fragment is due to a tryptophyl residue that is probably located near the S–Hg–S bond.

The difference spectrum of the C_L-Hg fragment in the presence of 4 M Gdn-HCl vs. the fragment in its absence had negative peaks at 286 and 295 nm (not shown). The values of $\Delta\epsilon$ at 286 and 295 nm were about −1000 and −1500 cm^{-1} M^{-1}, respectively.

Analytical Gel Filtration. The sizes of the intact C_L fragment and its modified forms were determined by gel chromatography on a Sephadex G-75 column. The calibration of the column was carried out with nine standard proteins with known Stokes radii (R_S). In Figure 7 the Stokes radii for the standard proteins are plotted against the inverse error function of $(1 - K_d)$, erf^{-1} $(1 - K_d)$, according to the method proposed by Ackers (1967). There was a linear relationship between the Stokes radii of the standard proteins and the inverse error functions of $(1 - K_d)$. Then the inverse error functions of $(1 - K_d)$ for the C_L fragment and its modified forms were plotted on the standard curve, and their Stokes radii were estimated. The Stokes radius of the intact C_L fragment was found to be 18 Å, which is almost the same as the value (17 Å) reported by Karlsson et al. (1972). The Stokes radii of the reduced C_L, C_L-Hg, and reduced and alkylated C_L fragments were found to be 18, 19, and 24 Å, respectively (Table I). We also determined the Stokes radii by the method of plotting the Stokes radius against the value of $K_d^{1/3}$ (Siegel & Monty, 1966). The standard curve was linear and gave the same Stokes radii for the C_L fragment and its modified forms.

Unfolding by Gdn-HCl and Heat. The results described above indicate that the β-sheet structure is disturbed in the C_L-Hg fragment but that its conformation is as compact as that of the intact C_L or reduced C_L fragment. In order to understand the effect on the stability of replacement of the S–S bond by the S–Hg–S bond, we measured the unfolding equilibria of the C_L-Hg fragment by Gdn-HCl and heat. Figure 8 shows the unfolding by Gdn-HCl measured by fluorescence change at 350 nm. The fluorescence intensity in water was 25% of the intensity in 4 M Gdn-HCl. The unfolding was reversible, and a cooperative transition with an apparent midpoint of 0.3 M Gdn-HCl was observed. We have

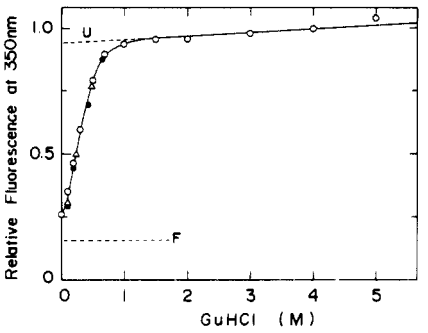

FIGURE 8: Relative fluorescence intensity at 350 nm of the C_L-Hg fragment as a function of Gdn-HCl concentration at pH 7.5 and 25 °C. Open circles represent the fluorescence intensities obtained on addition of Gdn-HCl to the C_L-Hg fragment prepared in water. Solid circles represent the fluorescence intensities obtained by dilution from 3 M Gdn-HCl of the C_L-Hg fragment prepared in water. Triangles represent the fluorescence intensities of the C_L-Hg fragment prepared in 3 M Gdn-HCl in the presence of 2 equiv of mercuric ions. The solid line indicates the theoretical curve for the unfolding transition constructed by using eq 2 and the values of $\Delta G_U^{H_2O}$ = 1.4 kcal/mol and Δn = 21.

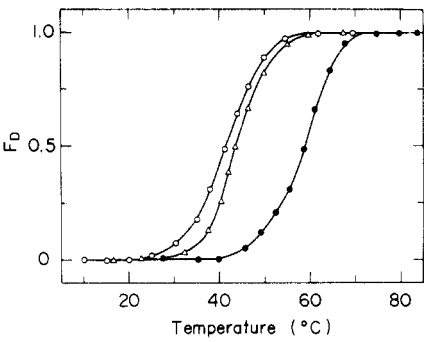

FIGURE 9: Thermal unfolding curve of the C_L-Hg (○), intact C_L (●), and reduced C_L (△) at pH 7.5. F_D is the fraction of unfolded protein.

previously reported the stabilities of the intact C_L and reduced C_L fragments under the same conditions (Goto & Hamaguchi, 1979). The stability of the C_L-Hg fragment was low compared with the intact C_L fragment (midpoint of 1.2 M Gdn-HCl) but was comparable to that of the reduced C_L fragment (midpoint of 0.4 M Gdn-HCl). We titrated the SH groups of the C_L-Hg fragment with DTNB in the presence of 4 M Gdn-HCl, but no SH group was titrated. This shows that the S–Hg–S bond remains intact in the unfolded protein. The C_L-Hg fragment was also prepared in 3 M Gdn-HCl in the presence of 2 mol of mercuric ion/mol of the reduced C_L fragment. When the concentration of Gdn-HCl was then lowered by dilution, the fluorescence intensity decreased. The equilibrium values of the fluorescence obtained by dilution of the C_L-Hg fragment prepared in 3 M Gdn-HCl were the same as the values obtained by the addition of Gdn-HCl to the C_L-Hg fragment prepared in the absence of Gdn-HCl (Figure 8). This shows that there is no difference in conformation and stability between the C_L-Hg fragment prepared in the presence of Gdn-HCl and then refolded and the fragment prepared in the absence of Gdn-HCl.

We also measured the unfolding of the C_L-Hg fragment by Gdn-HCl at 13 °C (not shown). The unfolding transition was similar to the transition at 25 °C, but the relative fluorescence intensity in water was 20% of that in 4 M Gdn-HCl and the midpoint of unfolding was 0.4 M Gdn-HCl.

Figure 9 shows the thermal unfolding of the C_L-Hg, intact C_L, and reduced C_L fragments. The midpoints of the thermal unfolding for the C_L-Hg, intact C_L, and reduced C_L fragments were 41, 60, and 43 °C, respectively.

Discussion

Reaction of the Reduced C_L Fragment with Mercuric Ions. To understand the role of the intrachain disulfide bond in the conformation and stability of the C_L fragment, the C_L fragment in which the disulfide bond is replaced by an S–Hg–S bond was prepared and its properties were studied. On the basis of the results of changes in tryptophyl fluorescence intensity and SH content with the concentration of mercuric ions (Figure 2), it was established that 1 mol of mercuric ion reacts with the pair of SH groups in the reduced C_L fragment. It is known that two sulfhydryl groups (RSH) are linked by a mercuric ion according to the reactions RSH + $HgCl_2$ ⇌ RSHgCl + H^+ + Cl^- and RSHgCl + RSH ⇌ RSHgSR + H^+ + Cl^- (Edsall & Wyman, 1958). Thus it is certain that the S–Hg–S bond is formed through the two SH groups in the reduced C_L fragment. The two cysteinyl residues of the reduced C_L fragment are buried in the interior of the molecule (Goto & Hamaguchi, 1979). Nevertheless, the SH groups react with a mercuric ion and the S–Hg–S bond is formed. The mechanism by which mercuric ions react with the buried SH groups was clarified by studying the kinetics of the reaction. The reaction proceeds slowly with an apparent first-order rate constant of 1.1 × 10^{-3} s^{-1} at pH 7.5 and 25 °C (Figure 3), and the kinetics are independent of the concentration of mercuric ions. Previously we studied the reaction of the SH groups in the reduced C_L fragment with DTNB (Goto & Hamaguchi, 1979), the formation of the disulfide bond from the reduced C_L fragment in the presence of glutathione (Goto & Hamaguchi, 1981), and the kinetics of the folding of the reduced C_L fragment (Goto & Hamaguchi, 1982b). All the results of these studies showed that there is a conformational equilibrium between a closed form of the protein in which the two SH groups are buried and an open form in which the SH groups are exposed and that the unfolding reaction from the closed form to the open form has a rate constant of 1 × 10^{-3} s^{-1} at pH 7.5 and 25 °C. This value is the same as the value of the rate constant for the reaction of the SH groups in the reduced C_L fragment with mercuric ions. Therefore the reaction of the SH groups with mercuric ions is rate-limited by the unfolding of the reduced C_L fragment and proceeds in the open form.

The validity of this mechanism was supported by the results obtained for the reaction of the reduced C_L fragment with mercuric ions in 3 M Gdn-HCl. As shown in Figure 2, even in the unfolded state, 1 mol of mercuric ion reacts specifically with 2 mol of SH group. This indicates that in the presence of 3 M Gdn-HCl formation of the derivative with the intrachain S–Hg–S bond is preferred to the formation of a derivative with two mercuric atoms in the form $(-S-Hg^+)_2$. Furthermore, there is no difference in the conformation and stability between the C_L-Hg fragment prepared in water and the C_L-Hg fragment prepared in 3 M Gdn-HCl and then refolded. The preferred formation of the S–Hg–S bond in the unfolded state may be explained simply if we consider the effective concentration (Creighton, 1983) of the SH groups in the reduced C_L fragment in the unfolded state. We previously determined the rate constants of the intra- and intermolecular thiol–disulfide interchange reactions of the reduced C_L fragment with glutathione (Goto & Hamaguchi, 1981). On the basis of these rate constants, the effective concentration of the SH groups in the unfolded state in 8 M urea is calculated to be 3.6 mM. This value is much greater than the concentration of mercuric ions used in the present experiments (5–30 μM). Therefore, an intermediate formed

during the reaction, in which one of the two cysteinyl residues forms a linkage with a mercuric ion while the other remains free, should form exclusively the intramolecular S–Hg–S bond.

Conformation of the C_L-Hg Fragment. The far-ultraviolet CD spectrum of the C_L-Hg fragment (Figure 5) suggests that the β-sheet of the C_L fragment is disturbed by the introduction of the S–Hg–S bond, although we cannot rule out the possibility that the large CD change in the aromatic absorption region contributes to the CD in the far-ultraviolet region (Adler et al., 1973). We failed to construct the CD spectrum in the far-ultraviolet region using the standard curves for α-helix, β-structure, and disordered structure given by Chang et al. (1978), but the spectrum suggests that the contents of α-helix and β-structure are small.

The intrachain disulfide bond of the intact C_L fragment is buried in the interior of the molecule. As shown in Figure 4, the first-order rate constant (0.02 s^{-1} at pH 7.5 and 25 °C) for the reduction with DTT of the S–Hg–S bond in the C_L-Hg fragment is independent of the concentration of DTT. This indicates that the S–Hg–S bond is also buried in the interior of the C_L-Hg fragment.

The C_L fragment contains two tryptophyl residues, and X-ray crystallographic studies (Davies et al., 1975; Amzel & Poljak, 1979) show that one of them is located close to the intrachain disulfide bond while the other is near the surface of the protein molecule. The following observations indicate that, as in the case of the intact C_L fragment, one of the two tryptophyl residues is located near the S–Hg–S bond in the interior of the C_L-Hg fragment molecule. (1) The CD bands in the aromatic absorption region of the C_L-Hg fragment were very large and disappeared upon unfolding by 4 M Gdn-HCl (Figure 5). This suggests that one tryptophyl residue is fixed in a specific conformation. (2) The tryptophyl fluorescence of the reduced C_L fragment was greatly quenched on reaction with mercuric ions (Figures 1 and 2; Table I), and the quenching was removed on unfolding of the C_L-Hg fragment (Figure 8). The S–Hg–S bond is known to have a great quenching effect on the tryptophyl fluorescence (Arnon & Shapira, 1969). As described above, the S–Hg–S bond in the C_L-Hg fragment is buried in the interior of the protein molecule. These findings indicate that there is a tryptophyl residue located near the S–Hg–S bond that is quenched by the bond. The fluorescence spectrum of the C_L-Hg fragment had a maximum at 335 nm (Figure 1). Although this maximum wavelength was longer than those of the intact C_L and reduced C_L fragments by 10 and 5 nm, respectively, it was shorter by 15 nm than that of the unfolded protein (Table I). This indicates that the tryptophyl residue is located in the interior hydrophobic region. (3) The magnitude of the blue shift at around 292 nm observed in the difference spectrum between the two proteins under different conditions gives a measure of the extent of exposure to an aqueous environment of tryptophyl residues from the interior hydrophobic region of the protein molecule. The value of $\Delta\epsilon$ at 292 nm in the difference spectrum of the C_L-Hg fragment vs. intact C_L fragment, which was constructed by using the spectrum shown in Figure 5 and the difference spectrum of the intact C_L vs. reduced C_L fragment (Goto & Hamaguchi, 1979), was very small. This indicates that the introduction of the S–Hg–S bond does not change greatly the hydrophobicity around the tryptophyl residues in the C_L fragment. The value of $\Delta\epsilon$ at 295 nm in the difference spectrum produced by unfolding of the C_L-Hg fragment was found to be −1500 M^{-1} cm^{-1}. This value is near the value expected for the transfer of one tryptophyl residue from the interior hydrophobic region of the protein molecule to an aqueous environment (Hamaguchi & Kurono, 1963). (4) The difference spectrum of the C_L-Hg fragment vs. reduced C_L fragment had a large positive peak at 300 nm (Figure 6). The absorption spectrum of the S–Hg–S bond obtained by measuring the absorption of reduced glutathione in the presence of mercuric ions against the absorption of reduced glutathione showed no peak at around 300 nm. Thus the peak at 300 nm observed for the difference spectrum of the C_L-Hg fragment vs. reduced C_L fragment was due to tryptophyl absorption being affected by the S–Hg–S bond. All these findings described above indicate that one of the two tryptophyl residues is located in the interior of the C_L-Hg fragment molecule, as it is in the intact C_L fragment.

As shown in Table I, the Stokes radii of the intact C_L, reduced C_L, and C_L-Hg fragments are very similar. This shows that the conformation of the C_L-Hg fragment, as well as that of the reduced C_L fragment, is as compact as that of the intact C_L fragment. On the other hand, the Stokes radius of the reduced and alkylated C_L fragment is much larger than those of the others. The Stokes radius of the reduced and alkylated C_L fragment in the random coil form was calculated to be 30 Å by using the equation for the intrinsic viscosity of the unfolded protein in concentrated Gdn-HCl solution (Tanford et al., 1967), $[\eta] = 0.716n^{0.66}$, where n is the number of residues, and eq 1. This was 6 Å longer than the observed value, indicating that the conformation of the reduced and alkylated C_L fragment is close to, but not the same as, that of the random coil.

As described above, the tryptophyl residue that is located near the disulfide bond buried in the intact C_L fragment molecule is also found near the S–Hg–S bond buried in the C_L-Hg fragment, with a similar degree of compactness in each. As described elsewhere, the kinetics of unfolding and refolding of the C_L-Hg fragment are also very similar to those of the intact C_L fragment. These findings suggest that the folding pattern of the polypeptide chain in the C_L-Hg fragment is similar to that of the intact C_L fragment.

The intrachain disulfide bonds in immunoglobulin domains are unusually long (Thornton, 1981; Richardson, 1981). While the distances between the α-carbons of the two cysteine residues of most disulfide bonds lie between 4.8 and 6.6 Å, those for immunoglobulins are between 6.6 and 7.4 Å. The conformation of the disulfide bond is described by five side-chain dihedral angles (χ_1, χ_2, χ_3, χ_2', and χ_1'). The dihedral angles χ_2, χ_3, and χ_2' for typical disulfide bonds are gauche–gauche–gauche (±90°, ±90°, ±90°). In contrast, those for the disulfides in immunoglobulins are trans–gauche–trans (180°, ±90°, 180°), and this produces the long C_α separation. In the case of the C_L domain, the dihedral angles are χ_1 = −171°, χ_2 = 173°, χ_3 = −95°, χ_2' = −169°, and χ_1' = 178°, the C_α separation for the two cysteinyl residues being 6.8 Å and the S–S separation being 2.3 Å (Saul et al., 1978). When the disulfide bond is reduced, the minimum S–S separation becomes 3.7–5.2 Å depending on the direction of the hydrogen atoms attached to the sulfur atoms, and the change in side-chain volume is calculated to be about 12 $Å^3$ assuming that the van der Waals radii of S and H atoms are 1.85 and 1.2 Å, respectively, and the covalent bond radii of S and H atoms are 1.04 and 0.37 Å (Pauling, 1960). In fact, however, there is no significant difference in conformation between the reduced C_L and intact C_L fragments (Goto & Hamaguchi, 1979; Ashikari et al., 1985). The S–Hg–S bond is linear, and the distance between the two sulfur atoms is 4.9 Å (Bradley & Kunchur, 1965), which is about 2.5 Å longer than that for the S–S bond. The van der Waals radius of the mercury atom

is 1.5 Å (Bondi, 1964), and the volume change is calculated to be 17 Å^3, which is not so different from the volume change caused by the reduction of the disulfide bond. Nevertheless, the conformation of the C_L-Hg fragment is different from that of the reduced C_L fragment.

The two SH groups in the reduced C_L fragment may be accommodated into the characteristic immunoglobulin folding by keeping the distance between the C_α carbons of the two cysteinyl residues unchanged by altering the dihedral angles χ_1, χ_2, χ_2', and χ_1'. The long distance between the C_α carbons of the disulfide may also be responsible for the absence of any great conformational change with reduction of the disulfide. The S–Hg–S bond is longer by 2.5 Å than the S–S bond, and the bond angle C_β–S–Hg (106°) is greater by about 15° than the bond angle C_β–S–S (about 90°). The entire group of C_β–S–Hg–S–C_β atoms becomes coplanar, while the dihedral angle χ_3 in C_β–S–S–C_β is −95° and the atoms do not become coplanar (Bradley & Kunchur, 1965). It may thus be difficult to maintain an unchanged C_α separation only by changing the dihedral angles χ_1 and χ_2, and the secondary structure characteristic of the C_L domain may be disturbed.

Stability of the C_L-Hg Fragment. Previously we measured the Gdn-HCl unfolding equilibria of the intact C_L and reduced C_L fragments and estimated the free energy changes ($\Delta G_U^{H_2O}$) for the unfolding reactions in the absence of denaturant assuming the two-state approximation for the transition and using the equation proposed by Tanford (1970) (Goto & Hamaguchi, 1979)

$$\Delta G_U = \Delta G_U^{H_2O} - \Delta nRT \ln (1 + ka_\pm) \qquad (2)$$

where Δn is the difference in the number of binding sites between the unfolded and folded states, k is the average binding constant of the sites, and $a_\pm$ is the mean ion activity of Gdn-HCl. We used 0.6 M^{-1} as the value of k.

We analyzed the Gdn-HCl unfolding equilibrium of the C_L-Hg fragment in the same way. In this analysis, the fluorescence intensity of the C_L-Hg fragment in the folded state was assumed to be 20% of the intensity in 4 M Gdn-HCl. This assumption was based on the observations that the value of $[\theta]$ at 270 nm is constant below 20 °C (Figure 9) and that the relative fluorescence intensity of the C_L-Hg fragment at 13 °C is 20% of the intensity in 4 M Gdn-HCl. The values of $\Delta G_U^{H_2O}$ and Δn of the C_L-Hg fragment were found to be 1.4 kcal/mol and 21, respectively. The value of $\Delta G_U^{H_2O}$ for the C_L-Hg fragment is comparable with that (1.6 kcal/mol) for the reduced C_L fragment but is much lower than the value (5.7 kcal/mol) for the intact C_L fragment. The values of n, which gives a measure of the cooperativity of unfolding, for the C_L-Hg fragment (21) and the reduced C_L (20) are similar. A similar tendency was also observed for the thermal stabilities of these proteins. The midpoint temperature for the C_L-Hg fragment (41 °C) is near that for the reduced C_L fragment (43 °C) but is much lower than that of the intact C_L fragment (60 °C).

From comparison of the stabilities to Gdn-HCl of the intact C_L and reduced C_L fragments, the contribution of the intrachain disulfide bond to the stability is estimated to be 4 kcal/mol. The increase in the stability created by the presence of the disulfide bond has been explained in terms of the larger conformational entropy of the reduced C_L fragment compared with the entropy of the intact C_L fragment in the unfolded state (Goto & Hamaguchi, 1979). In the C_L-Hg fragment the same loop as in the intact C_L fragment is formed by the S–Hg–S bond, and it remains intact even in the unfolded state. Therefore, we can assume that the free energies contributed by the conformational entropies of these unfolded proteins are the same and that the difference in stability between the intact C_L and C_L-Hg fragments should be ascribed to the difference in free energy between the proteins in the folded state. The difference in free energy of unfolding in water is estimated to be about 4.5 kcal/mol. This value corresponds to the strain produced by the replacement of the S–S bond by the S–Hg–S bond in the C_L fragment.

Registry No. Mercury, 7439-97-6.

REFERENCES

Ackers, G. K. (1967) *J. Biol. Chem. 242*, 3237–3238.

Adler, A. J., Fasman, G. D., & Greenfield, N. (1973) *Methods Enzymol. 27*, 712–735.

Amzel, L. M., & Poljak, R. L. (1979) *Annu. Rev. Biochem. 48*, 961–997.

Arnon, R., & Shapira, E. (1969) *J. Biol. Chem. 244*, 1033–1038.

Ashikari, Y., Arata, Y., & Hamaguchi, K. (1985) *J. Biochem. (Tokyo) 97*, 517–528.

Bondi, A. (1964) *J. Phys. Chem. 68*, 441–451.

Bradley, D. C., & Kunchur, N. R. (1965) *Can. J. Chem. 43*, 2786–2792.

Chang, C. T., Wu, C. S. C., & Yang, J. T. (1978) *Anal. Biochem. 91*, 13–31.

Creighton, T. E. (1983) *Biopolymers 22*, 49–58.

Davies, D. R., Padlan, E. A., & Segal, D. M. (1975) *Annu. Rev. Biochem. 44*, 639–667.

Edsall, J. T., & Wyman, J. (1958) in *Biophysical Chemistry*, Vol. I, pp 63–64, Academic, New York.

Ellman, G. L. (1958) *Arch. Biochem. Biophys. 82*, 70–77.

Gething, M. J. H., & Davidson, B. E. (1972) *Eur. J. Biochem. 30*, 352–353.

Goto, Y., & Hamaguchi, K. (1979) *J. Biochem. (Tokyo) 86*, 1433–1441.

Goto, Y., & Hamaguchi, K. (1981) *J. Mol. Biol. 146*, 321–340.

Goto, Y., & Hamaguchi, K. (1982a) *J. Mol. Biol. 156*, 891–910.

Goto, Y., & Hamaguchi, K. (1982b) *J. Mol. Biol. 156*, 911–926.

Goto, Y., Azuma, T., & Hamaguchi, K. (1979) *J. Biochem. (Tokyo) 85*, 1427–1438.

Hamaguchi, K., & Kurono, A. (1963) *J. Biochem. (Tokyo) 54*, 111–122.

Karlsson, F. A., Peterson, P. A., & Berggård, I. (1972) *J. Biol. Chem. 247*, 1065–1073.

Le Maire, M., Rivas, E., & Moller, J. V. (1980) *Anal. Biochem. 106*, 12–21.

Pauling, L. (1960) in *The Nature of the Chemical Bond*, 3rd ed., pp 224, 260, Cornell University Press, Ithaca, NY.

Richardson, J. S. (1981) *Adv. Protein Chem. 31*, 167–339.

Saul, F. A., Amzel, L. M., & Poljak, R. L. (1978) *J. Biol. Chem. 253*, 585–597.

Siegel, L. M., & Monty, K. J. (1966) *Biochim. Biophys. Acta 112*, 346.

Squire, P. G., & Himmel, M. E. (1979) *Arch. Biochem. Biophys. 196*, 165–177.

Sumi, A., & Hamaguchi, K. (1982) *J. Biochem. (Tokyo) 92*, 823–833.

Tanford, C. (1968) *Adv. Protein Chem. 23*, 121–217.

Tanford, C. (1970) *Adv. Protein Chem. 24*, 1–95.

Tanford, C., Kawahara, K., & Lapanje, S. (1967) *J. Am. Chem. Soc. 89*, 729–736.

Thornton, J. M. (1981) *J. Mol. Biol. 151*, 261–287.